

## Electronic supplementary information

### Construction of CF@Cu<sub>x</sub>O/FeCoO nanowire arrays with an optimized bandgap to facilitate photo-assisted electrocatalytic water splitting

Xiankui Lv,<sup>a</sup> Qian Rong,<sup>a\*</sup> Muhammad Arif,<sup>a</sup> Jing Xie,<sup>ac</sup> Amjad Nisar,<sup>b</sup> Mashkoor Ahmad,<sup>b</sup> Weibin Zhang,<sup>a</sup> and Ting Zhu<sup>a\*</sup>

<sup>a</sup> School of Physics and Electronic Information, Yunnan Key Laboratory of Optoelectronic Information Technology, Yunnan Normal University, 768 Juxian Street, Kunming 650500, Yunnan, China.

<sup>b</sup> Nanomaterials Research Group, Physics Division, PINSTECH, Islamabad 44000, Pakistan.

<sup>c</sup> School of Materials Science and Engineering, Central South University, 932 Lushan Road South, Changsha 410083, Hunan, China.

\*Emails: 18487271435@163.com (Q. Rong); zhut0002@ynnu.edu.cn (T. Zhu)

## S1. Characterizations and DFT calculation

In this study, all calculations were based on the density functional theory (DFT) and implemented using the Vienna Atomic Number Simulation Package (VASP). The exchange-correlation interaction between electrons was described by the Perdew-Burke-Ernzerhof (PBE) functional under the generalized gradient approximation (GGA). The interaction between electrons and ions was treated by the projector augmented wave (PAW) method, which was embedded in atomic pseudopotentials. The cut-off energy of the plane wave was set to 400 eV to ensure calculation accuracy. During the geometry optimization process, the k-point grid adopts  $3 \times 2 \times 1$  gamma point distribution. The convergence criterion of the optimization process is that the energy change of each atom does not exceed  $1.0 \times 10^{-5}$  eV and the maximum interatomic force does not exceed  $5.0 \times 10^{-2}$  eV/Å.

In the optimized cubic phase Cu<sub>2</sub>O unit cell, the lattice parameters were  $a = b = c = 4.26$  Å, belonging to the Pn-3m space group. The crystal structure consists of 4 Cu atoms and 2 O atoms. The optimized Co<sub>3</sub>O<sub>4</sub> unit cell exhibits cubic symmetry with lattice constant  $a = b = c = 7.97$  Å, belonging to FD-3M space group, and contains 24 Co atoms and 32 O atoms. Based on these two species, a Cu<sub>2</sub>O/Co<sub>3</sub>O<sub>4</sub> heterojunction was constructed. The Cu<sub>2</sub>O (110) plane consists of 48 atoms with lattice parameters of  $a = 8.53$  Å and  $b = 12.07$  Å, while the Co<sub>3</sub>O<sub>4</sub> (220) plane comprises 56 atoms with lattice parameters of  $a = 7.97$  Å and  $b = 11.27$  Å. During the construction of the heterojunction, doping modification was achieved by replacing one Co atom in the Co<sub>3</sub>O<sub>4</sub> lattice with an Fe atom. A new surface model perpendicular to the lateral plane of Cu<sub>x</sub>O/FeCoO heterojunction was constructed. To eliminate the effects of periodic boundary conditions, a vacuum layer with a thickness of 15 Å was introduced in all surface models. This design ensures the accuracy of the model during simulations while preventing interactions between adjacent periodic structures.

The adsorption energy ( $E_{ads}$ ) was positively correlated with adsorption intensity, that is, the larger the absolute value, the stronger the adsorption. The adsorption energies of H<sub>2</sub>O and \*OH on the substrate material were calculated by the following equations, respectively:

$$E_{ads} = E_{total} - E_{surface} - E_{H_2O}$$

$$E_{ads} = E_{total} - E_{surface} - E_{*OH}$$

Where  $E_{total}$  represents the total energy of the whole adsorption system after adsorption of H<sub>2</sub>O and \*OH,  $E_{surface}$  represents the pure surface without adsorption of any

substance, and  $E_{H_2O}$  and  $E_{*OH}$  were the energies of the isolated  $H_2O$  molecule and  $*OH$  group, respectively. By using the above formula, the energy change during the adsorption process can be quantitatively evaluated, thereby revealing the strength of the adsorption effect.

## S2. Supplementary figures

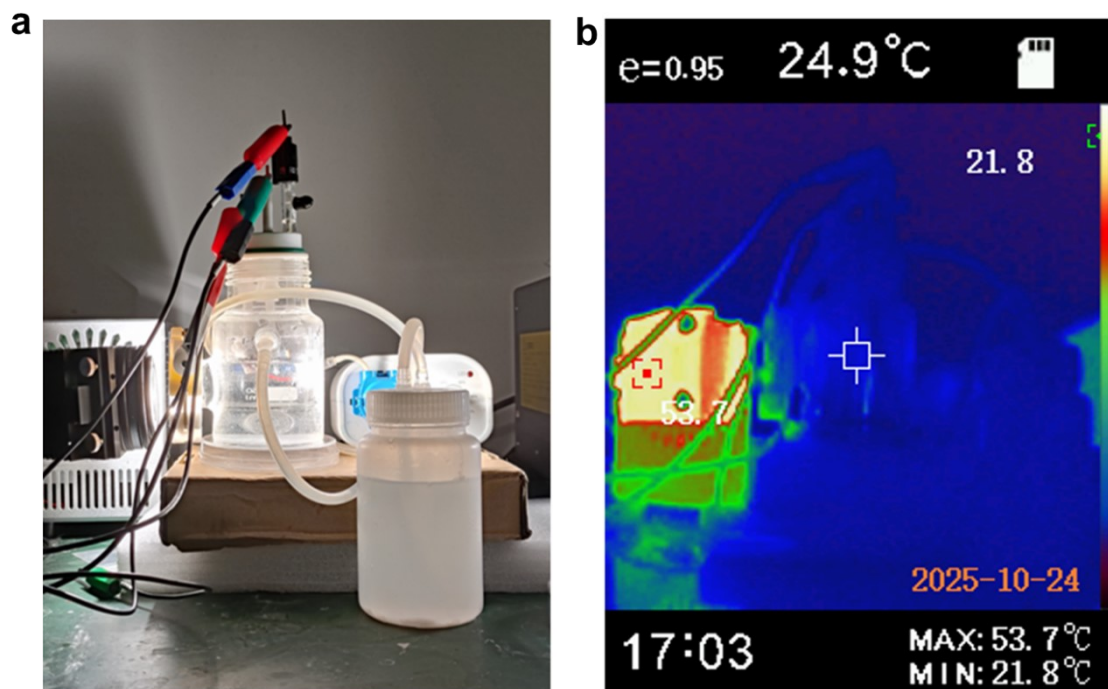


Fig. S1. A digital photo of the electrolytic cell device (a), and an infrared image capturing the temperature of the electrolyte (b).

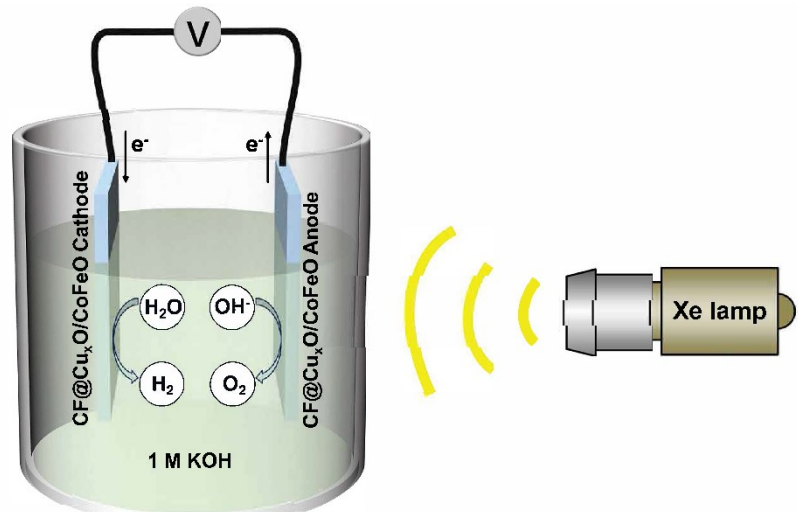


Fig. S2. Schematic diagram of light-assisted overall water splitting device.

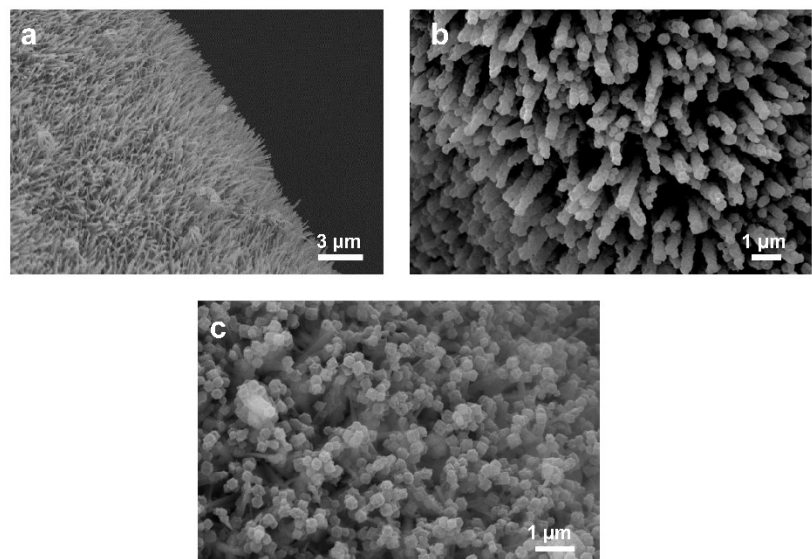


Fig. S3. The SEM images of CF@Cu(OH)<sub>2</sub> (a), CF@Cu(OH)<sub>2</sub>/ZIF67 (b), and CF@Cu(OH)<sub>2</sub>/Fe-ZIF67 (c) samples, respectively.

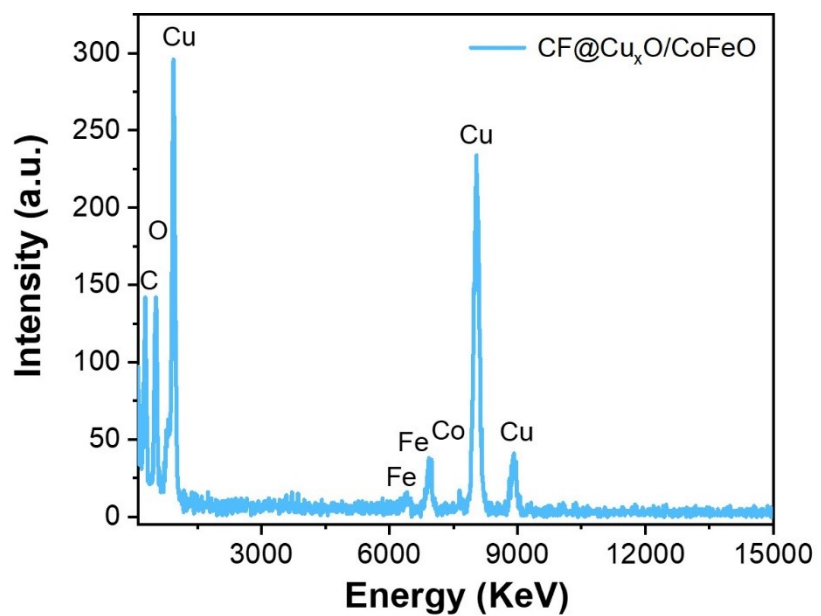


Fig. S4. EDS spectrum of CF@Cu<sub>x</sub>O/CoFeO nanowires.

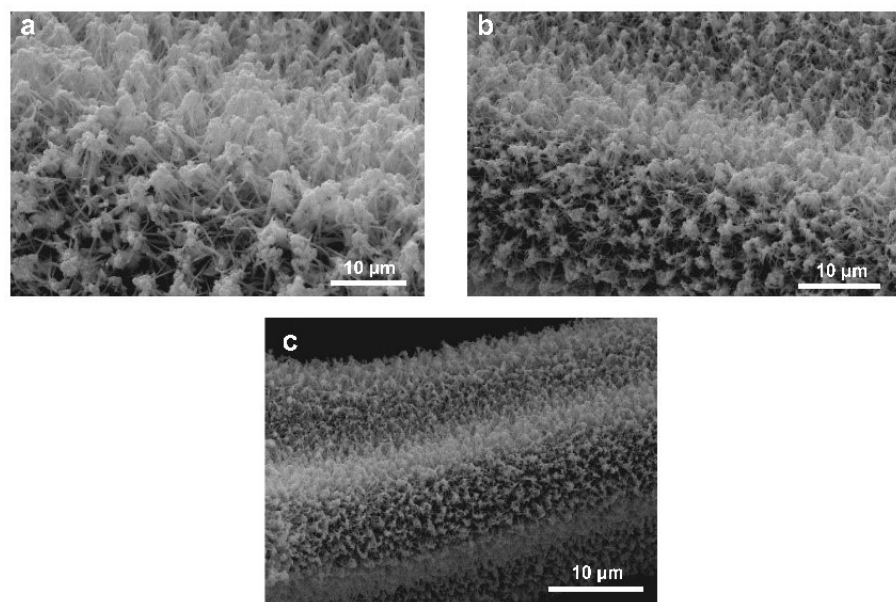


Fig. S5. Morphology of CF@Cu<sub>x</sub>O/CoFeO nanowire arrays after a 12 h cycling test for OER.

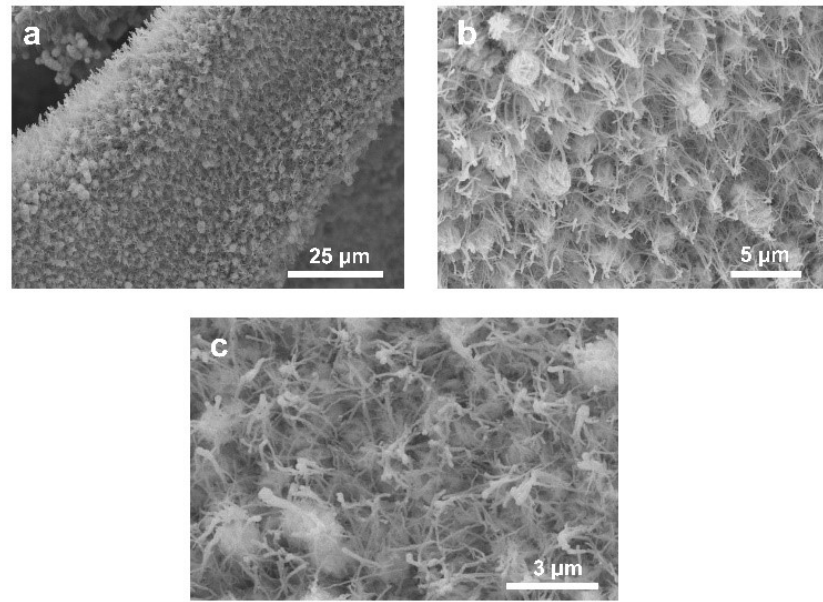


Fig. S6. Morphology of CF@Cu<sub>x</sub>O/CoFeO<sub>x</sub> nanowire arrays after a 12 h cycling test for HER.

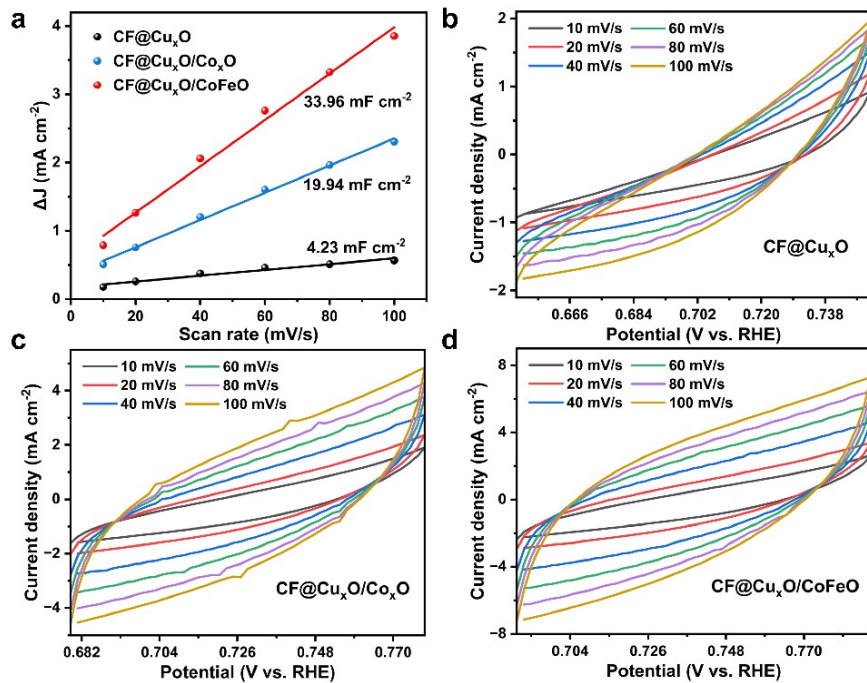


Fig. S7. Double-layer capacitance ( $C_{dl}$ ) (a), CV curves of CF@Cu<sub>x</sub>O (b), CF@Cu<sub>x</sub>O/Co<sub>x</sub>O (c), and CF@Cu<sub>x</sub>O/CoFeO (d) at different scan rates.

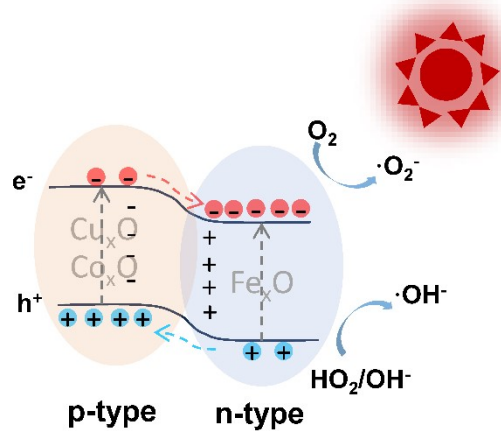


Fig. S8. Schematic diagram of energy level transition pathways and charge transfer in  $\text{Cu}_x\text{O}/\text{CoFeO}$ .

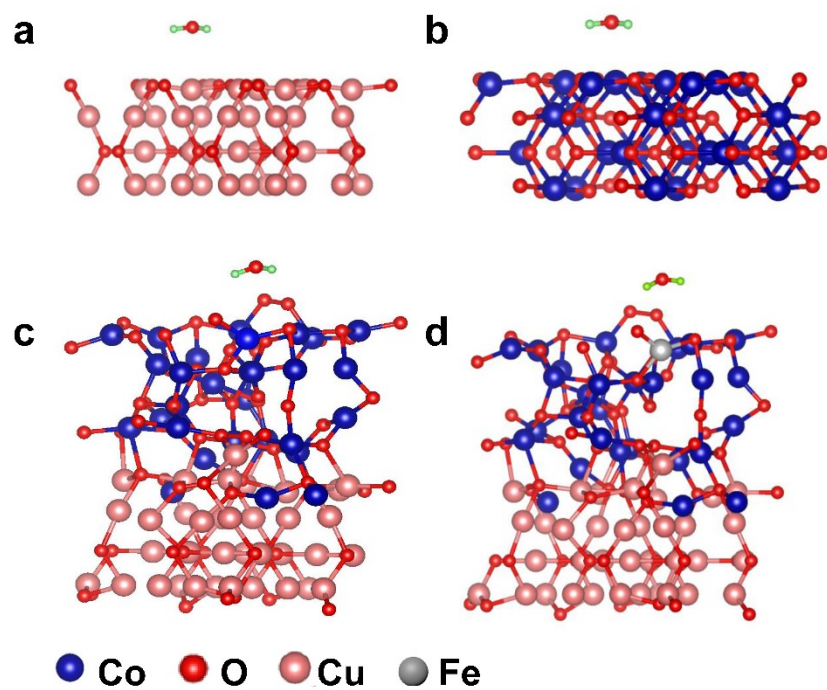


Fig. S9. Atomic structure models of  $\text{Cu}_x\text{O}$  (a),  $\text{Co}_x\text{O}$  (b),  $\text{Cu}_x\text{O}/\text{Co}_x\text{O}$  (c) and  $\text{Cu}_x\text{O}/\text{CoFeO}$  (d) for adsorbing  $\text{H}_2\text{O}$ .

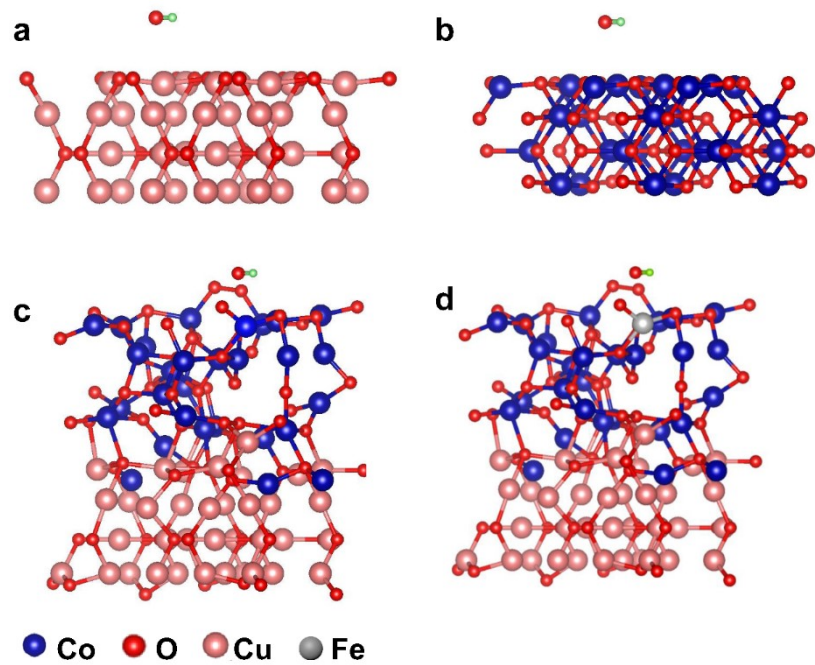


Fig. S10. Atomic structure models of Cu<sub>x</sub>O (a), Co<sub>x</sub>O (b), Cu<sub>x</sub>O/Co<sub>x</sub>O (c) and Cu<sub>x</sub>O/CoFeO (d) for adsorbing \*OH.

Table S1. The d-band values of Cu<sub>x</sub>O, Cu<sub>x</sub>O/Co<sub>x</sub>O and Cu<sub>x</sub>O/CoFeO

Sample	d-band values
Cu <sub>x</sub> O	-2.17 eV
Cu <sub>x</sub> O/Co <sub>x</sub> O	-1.81 eV
Cu <sub>x</sub> O/CoFeO	-1.79 eV